FRICTION CHARACTERISTICS BETWEEN THIN PLASTIC FILM AND STEEL ROLLER

By

Hiromu Hashimoto and Yuta Sunami
Tokai University
JAPAN

ABSTRACT

To establish the Roll-to-Roll Printed Electronics, which can be applied to manufacture the high functional thin film based devices, it is needed to combine the Roll-to-Roll transportation system and coating technology effectively. For that purpose one of important factors to be considered is the friction characteristics between the thin plastic film and steel roller. In past research, however, as far as authors know, there is no research which describes friction characteristics between thin plastic film and steel roller. In this paper, the static friction between the plastic film and steel roller was measured by pulley method while changing film thickness of film, roller surface roughness, web tension, and relative humidity. As a result, the static friction coefficient between thin film and steel roller was significantly influenced by film thickness and roller surface roughness, web tension and relative humidity have an effect on the static friction coefficient. From analysis of variance, it was confirmed statistically that contribution ratio of three factors, relative humidity, web tension and surface roughness which were 23.8 %, 32.6 % and 36.1 %, were very high.

INTRODUCTION

In recent years, a product development system for manufacturing of high functional thin film based devices such as flexible displays, thin-film solar cells, batteries and electric skins is being promoted. These devices are manufactured by Printed-Electronics (PE) manufacturing which is one of the most remarkable systems of manufacture at present. PE can manufacture a wide variety of flexible devices. However, the system is not yet capable of manufacturing mass products because of a high cost associated with making of large-area devices. On the other hand, Roll-to-Roll (R2R) transportation system has been applied to the manufacturing of thin and flexible materials which is called a web, such as plastic films, papers, thin metal plates at low cost. R2R system can transport the web using a large number of rollers. Several processes are performed on the web, such as recording, coating, drying, laminating during transportation of the web.

Therefore, it is needed to establish the new technology named Roll-to-Roll-Printed-Electronics (R2RPE) manufacturing system which combines with the R2R transportation system and PE manufacturing system as shown in Figure 1 to manufacture a large amount of high functional thin film based devices. However, the application of this system is being limited to the manufacturing of only a few devices because R2RPE manufacturing system has many problems. For example, as the manufacturing devices require high precision, registration is very important during the transportation of the web. During the web transports on rollers, web defects such as wrinkling, slippage, sagging, unwanted meandering on rollers can occur [1]-[2]. In order to prevent the defects, it is important to understand the friction characteristics between a web and rollers. In previous studies, the effect of the entrained air between a web and roller on friction characteristic was examined, in which the air film thickness was modeled by the foil bearing equation [3]-[11]. Hashimoto presented new theoretical modeling of friction coefficient between uncoated paper-web and steel roller under mixed lubrication by using contact mechanics, and the model was verified compared with the measured results [12]. However, higher accuracy of the transportation technology for the web is being required to establish the R2RPE manufacturing system. Therefore, it is necessary to investigate friction characteristics between the web and roller surface including effects of various factors in more detail. In particular, plastic film used for high functional devices is being thinner at present. However, the friction characteristics between the thin plastic film, which has several μm thickness, and roller surface has not been clarified yet.

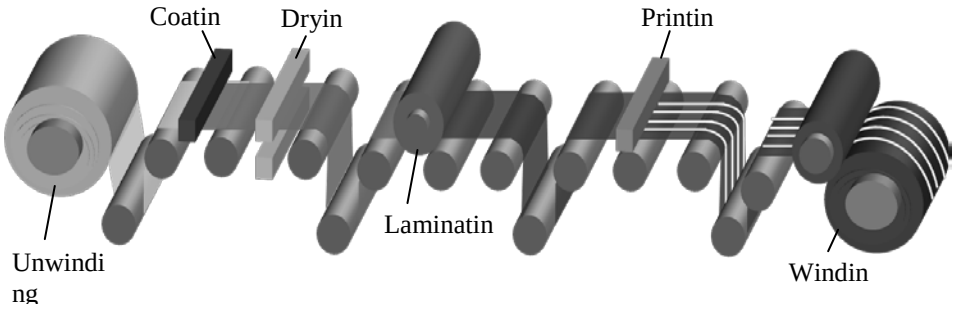

Figure 1－Roll-to-Roll-Printed-Electronics manufacturing system

In this paper, a fundamental experiment, in which the static friction force between plastic film and steel roller is measured, is conducted while changing film thickness, web tension, relative humidity of ambient air and roller surface roughness.

EXPERIMENTAL APPARATUS AND METHOD

Experimental apparatus and test rollers and films

Figure 2 shows the overview of the experimental apparatus for measuring the static friction force between the plastic film and steel roller surface. The experimental apparatus consists of a roller, test film, weight, isolation chamber and a humidifier and these components comprise a simple system in which a pulley method is implemented for friction measurement. The test roller was cylindrical which was fixed in the experiment. Three specimens of polyethylene terephthalate (PET) film were used in tests, each of a different thickness. Figure 3 and Figure 4 show the surface roughness of test rollers and films with the co-focused laser microscope. Table 1 and Table 2 show the specifications

of test rollers and films, respectively. In Figures 3 and 4, maximum height of surface roughness of test rollers is higher than for the test films. In Table 1 and Table 2, R_{ku} and R_{sk} indicate the kurtosis and skewness of roughness curve. As can be seen in Tables, the test rollers and films have qualitatively similar surface profile because of $R_{ku} < 0$, $R_{sk} < 3$. Figure 5 shows the probability density function of surface roughness of test rollers. As can be seen in these figures, the probability density function of surface roughness for all three rollers agrees closely with the normal distribution curve.

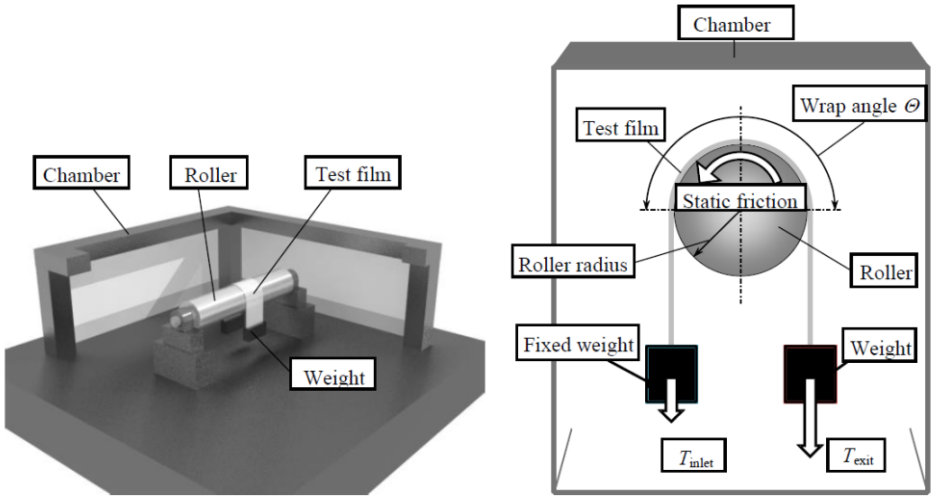

Figure 2 – Experimental apparatus

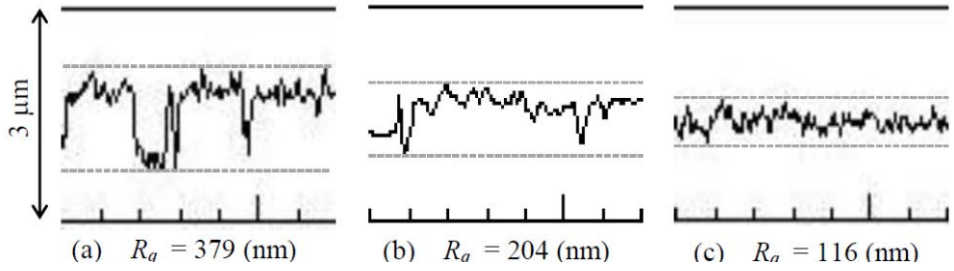

Figure 3 – Surface roughness profiles of test rollers

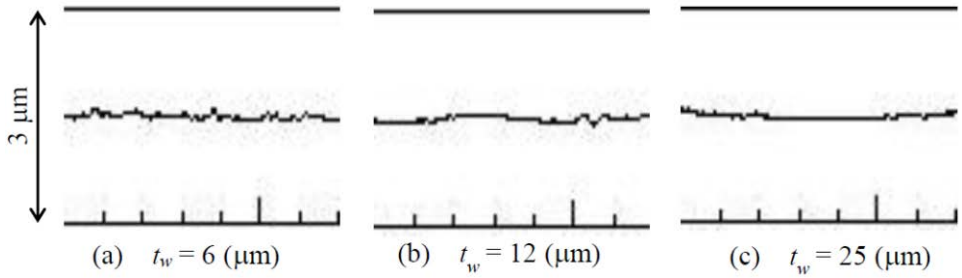

Figure 4 – Surface roughness profiles of test films

Parameter			Value		
			Roller A	Roller B	Roller C
Material			SCM-440		
Radius	r	(mm)	40		
Arithmetic average roughness	R_a	(nm)	284	182	89
Maximum roughness height	R_y	(nm)	4830	1950	1210
Ten points height roughness	R_z	(nm)	3218	1434	890
RMS roughness	R_q	(nm)	379	204	116
Skewness	R_{sk}		-0.12	-0.08	-0.03
Kurtosis	R_{ku}		1.02	0.81	1.18

Table 1 – Specifications of test rollers

Parameter			Value		
Thickness	t_w	(μm)	6	12	25
Width	W	(mm)	20		
Young's modulus (MD)	E_{MD}	(GPa)	7.59	4.91	4.34
Young's modulus (CD)	E_{CD}	(GPa)	4.06	5.43	4.65
Arithmetic average roughness	R_a	(nm)	25	28	34
Maximum roughness height	R_y	(nm)	300	450	380
Ten points height roughness	R_z	(nm)	238	280	160
RMS roughness	R_q	(nm)	32	37	39
Skewness	R_{sk}		-0.29	-0.21	-0.09
Kurtosis	R_{ku}		0.17	0.31	0.41

Table 2 – Specifications of test films

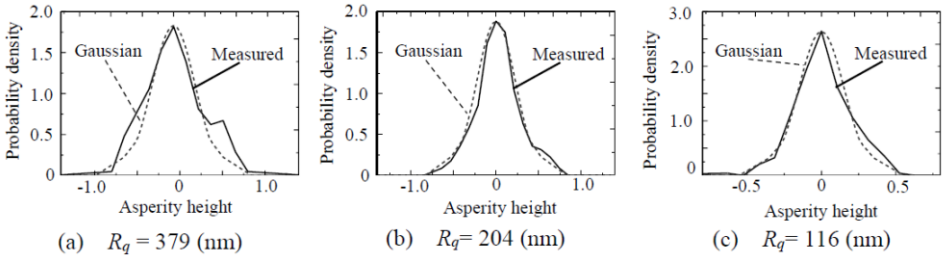

Figure 5 – Probability density function of test roller surface roughness

Experimental method

In this experiment, first a piece of the test film was put on the roller and then identical weights were set up at the ends of the film as shown in Figure 2 (b). After that, the weight (T_{exit}) was increased at one end of side by slowly adding water to a container suspended from film's end. The exit tension T_{exit} increase was continued until the test film started to slide on the test roller. After obtaining the inlet and exit tensions, the static

$$\mu_s = \frac{1}{\Theta} \ln\left(\frac{T_{\text{exit}}}{T_{\text{inlet}}}\right) \quad \{1\}$$

where Θ is wrap angle. In the experiment, wrap angle was determined as $\Theta=\pi$.

Furthermore, the relative humidity of ambient air was changed with a humidifier in increments of 5 % from 30 % to 80 %, and inlet tension was changed within range of T_{inlet} = 6, 12, 25 N/m.

In this experiment, static electricity is generated between the film and roller surface because a PET film is an insulator. To clarify the effect of the electrostatic force on the friction characteristics, a surface potential, *V*, on the film was measured with the surface electrometer. Measurement areas were three points of contact between the film and the roller surface. Surface potential was measured after measuring static friction force and changing the relative humidity. An electrostatic potential is generated between the surfaces of the film and the roller with the build up of the electric charge *Q* in the system. Electric charge *Q* is calculated by;

$$Q = CV \quad \text{(C)} \quad \{2\}$$

where *C* is electric capacitance which is obtained by;

$$C = \frac{\varepsilon_0 \varepsilon_r S}{t_w} \quad \text{(F)} \quad \{3\}$$

where ε_0 is electric permittivity of vacuum, ε_r is relative permittivity of PET film, *S* is area of apparent contact between the film and roller surface and t_w is film thickness, respectively. In the experiment, ε_0 is 8.854×10^{-12} F/m, ε_r is 3.2 and *S* is 2.51×10^{-3} m^2.

EXPERIMENTAL RESULTS

Influences of static electricity and film thickness

Figure 6 shows the relationship between the static friction coefficient and the surface potential for films of different thickness under the inlet tension of 12 N/m and temperature between 24.9~26.4 °C and with the relative humidity between 40.1~45.2 %. In the figure, the horizontal and vertical axes indicate the surface potential of the film and the static friction coefficient, respectively. This result shows that the surface potential was generated in the -1.5 to 0 kV range, and the static friction coefficients were not only slightly influenced by the surface potential. However, comparing the results with regard to the influence of the film thickness, the static friction coefficient in the case of thin film was higher than for the thick film.

Figure 7 shows the relationship between the static friction coefficient and the film thickness. The measurements were conducted 10 times to investigate the repeatability. As can be seen in the figure, the static friction coefficient was increased with the decrease in the film thickness. This results obtained are considered to be influenced by the electrostatic force and deformation of the film. When the electrostatic force is generated between the film and roller surface, then the film is deformed along with the roller

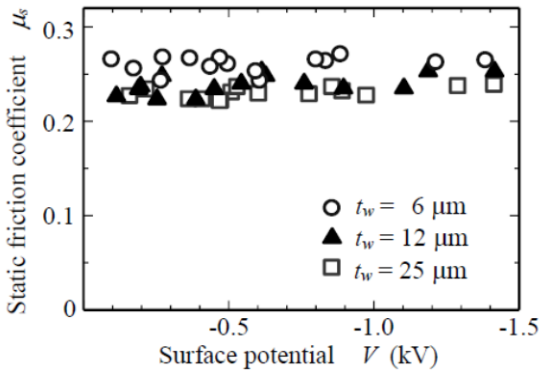

Figure 6 – Relationship between static friction coefficient and surface potential

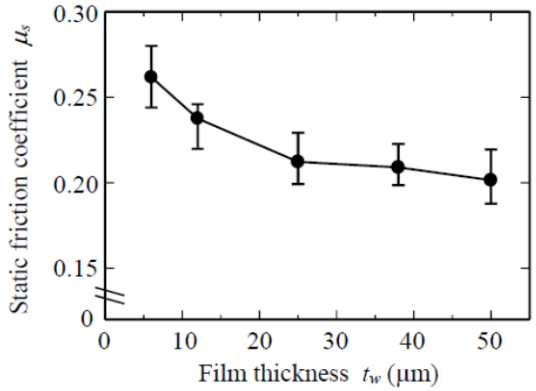

Figure 7 – Relationship between static friction coefficient and film thickness
(T_{inlet}=12 N/m, T=24.9~26.4°C, H=40.1~45.2%)

surface asperities. Moreover, the electric charge is inversely proportional to film thickness as shown in Equations {2} and {3}. It means that the electrostatic force is increased with a decrease in the film thickness. On the other hand, the bending stiffness of the film is proportional to the cube of the film thickness as shown in the following equation.

$$EI = \frac{t_w^3 W E_{MD}}{12} \quad (\mathrm{Nm}^2) \qquad \{4\}$$

where, W is the width of film, E_{MD} is Young's modulus of film.

As a result, thin film is deformed and sagged more, as compared to thick film due to electrostatic force and lower bending stiffness, and it covers more closely the roller surface asperities. When the film is pulled tangentially, the asperities behave as an anchor. The static friction coefficient in the case of thin film was increased than in the case of thick film due to "anchor effect" and "sagging effect" between the deformed film and asperities as shown in Figure 8.

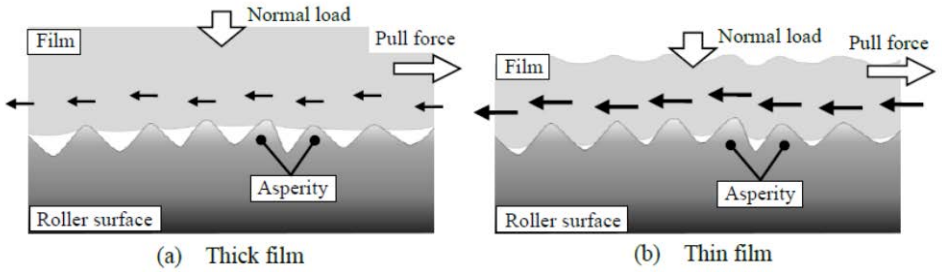

Figure 8 – An increase of resistance due to “anchor effect” and “sagging effect”

Influence of relative humidity

Figure 9 shows the relationship between the static friction coefficient and relative humidity for three film thicknesses, t_w = 6, 12, 25 μm, and three inlet tensions, T_{inlet} = 6, 12, 25 N/m under temperature was between 23.7~28.1 °C. The measurements were conducted 10 times to investigate the repeatability. In these figures, the plots and the error bar mean the average value and the variability, and the dash lines indicate trend line, respectively. In addition, the horizontal and vertical axes indicate relative humidity and static friction coefficient, respectively. It was confirmed that surface potential of test film used was obtained between -1.5~0 kV in the measurements. In these figures, the static friction coefficients of each film thickness were increased with an increase in relative humidity. In particular, the rate of the increase of the static friction coefficient was greater beyond the relative humidity of 60 %. The reason for this behavior is probably the influence by the meniscus force in contact area between the film and roller surface asperities.

Increasing the relative humidity causes the meniscus force generated between the surface asperities, and then the film is pulled to the roller surface. The contact area between the film and roller surface asperities is larger, and then deformation of the film increases. As a result, the static friction coefficient increases due to the anchor effect between the deformed film and asperities, similar to the results in Figure 7. The greater the increase of the relative humidity, the more the static friction coefficient is increased. In the humidity range from 70 % to 80 % in Figure 9 (a), measurement date was not obtained because the film would not slide. It was confirmed that the relative humidity strongly influences the static friction coefficient.

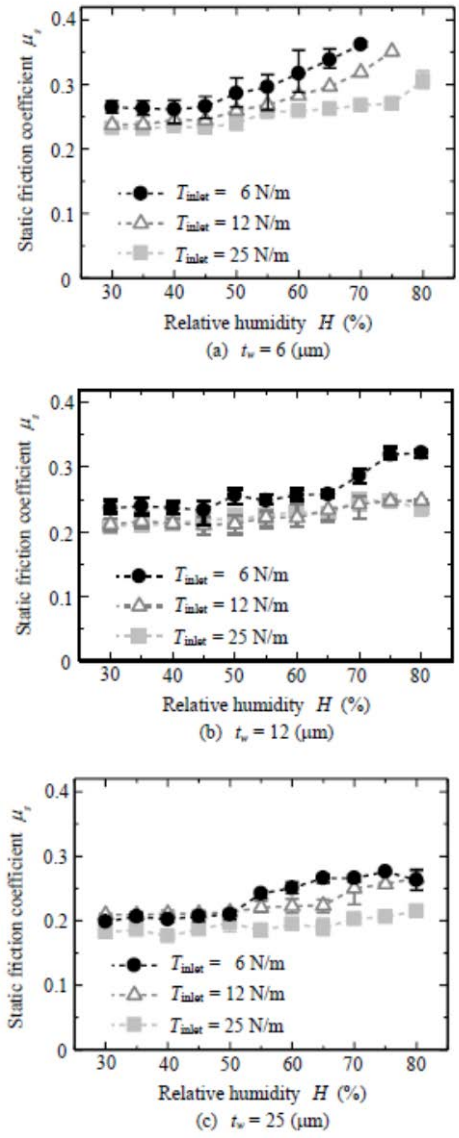

Figure 9 – Variation of static friction coefficient with relative humidity as a parameter of film inlet tension

To estimate the effect of meniscus force on static friction coefficient, contact angles, θ_{roller} and θ_{film}, between droplet (pure water) and test film, between droplet and test roller were measured with micro scope. The measurements were conducted 10 times. As a result, θ_{roller} and θ_{film} were 71.6 deg. and 57.6 deg.. Meniscus force F_m can be calculated by the following Young Equation;

$$F_m = 2\pi r_m \gamma \left(\theta_{roller} + \theta_{film}\right) \quad \text{(N)} \qquad \{4\}$$

where, r_m is curvature radius of meniscus, γ is surface tension of pure water.

Figure 10 shows the relationship between meniscus force and relative humidity. From the result, the meniscus force increases with an increase in relative humidity similar to the results of Figure 9. As a result, there is probably correlation between static friction force and relative humidity. Here, to confirm the relationship between static friction force and relative humidity, analysis of correlation was conducted for each film thickness. As a result, coefficients of correlation R_c of each film, t_w = 6, 12, 25 μm, were 0.95, 0.92 and 0.91, respectively. It was confirmed that static friction coefficient correlates strongly with relative humidity.

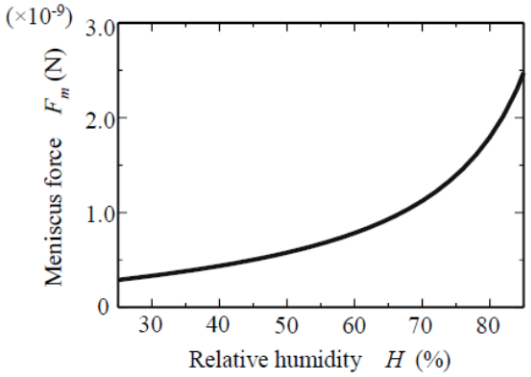

Figure 10 – Relationship between relative humidity and meniscus force

	H =30~50 (%)	H = 60~80 (%)
Film thickness	67.6	45.6
Web tension	22.1	22.4
Relative humidity	6.8	23.7

Table 3 – Results of analysis of variance

On the other hand, comparing the results of changing inlet tension, the static friction coefficient under low tension was more significantly increased with the increase in relative humidity. The static friction coefficient stays constant with an increase the inlet tension (applied load) according to the Amonton's-Coulomb's law. However, the different tendency, in which the static friction coefficient was increased with the decrease in the web tension, was shown probably due to strong anchor effect and sagging effect between the deformed film and roller surface asperities. Here, to confirm the relationship between static friction force and inlet tension, analysis of correlation was conducted for each film thickness in the case of relative humidity of 30 %, where is a relatively small influence of relative humidity. As a result, coefficients of correlation R_c of each film, t_w = 6, 12, 25 μm, were 0.83, 0.79 and 0.75, respectively. It was also confirmed that static friction coefficient correlates strongly with web tension.

In contrast, the influence of the relative humidity on the static friction coefficient was reduced with the increase with the film thickness and inlet tension as shown in Figure 9 (a)~(c). The sagging and deformation of the top of film are reduced due to higher bending stiffness, and then area of asperities covered by deformed film is reduced. Moreover, the tendency is probably more pronounced under high tension. As a result,

static friction coefficient was decreased due to lower anchor effect.

As shown above, the effect of relative humidity and web tension on static friction coefficient becomes higher in the case of using thin film. Therefore, analysis of variance was conducted to determine the contribution ratio of each factor to friction coefficient in relative humidity from 30 % to 50 % and from 60 % to 80 %, in which there is different tendency of increasing static friction coefficient as shown in Figure 9. Table 3 show the results of analysis of variance. As can be seen in the Table, contribution ratio of film thickness is higher than for other ratios. Moreover, the ratio of web tension is relatively independent of relative humidity. On the other hand, although the ratio of relative humidity is small under relative humidity in 30 % to 50 % range, the ratio is large under high humidity.

Influence of roller surface roughness

Figure 11 shows the relationship between static friction coefficient and relative humidity for three test rollers, R_q = 116, 204, 379 nm, three inlet tension T_{inlet} = 6, 12, 25 N/m using the film of 6 μm under temperature was between 24.7~25.5 °C. In the humidity of 80 % in Figure 11 (a), measurement date was not obtained because the film would not slide.

In these figures, the static friction coefficient of using roller with surface roughness of 116 nm were larger than for other results. From results, it was found that the decrease in the roller surface roughness has an effect of an increase in the static friction coefficient. In particular, the tendency is more pronounced under low tension and high relative humidity. The reason for this behavior is probably the influence by increasing the real contact area between the film and roller surface asperities. When the load is applied to the film, then the film is deformed along with the roller surface asperities. Moreover, the clearance between the film and steel roller was narrowed using the roller with smooth surface compared to the roller with rough surface as shown in Figure 12. As a result, real contact area is increased and it covers more closely the roller surface asperities, as compared to result of using the roller with rough surface. When the film is pulled tangentially, the asperities behave as an anchor. The static friction coefficient was increased due to “anchor effect” between the deformed film and asperities.

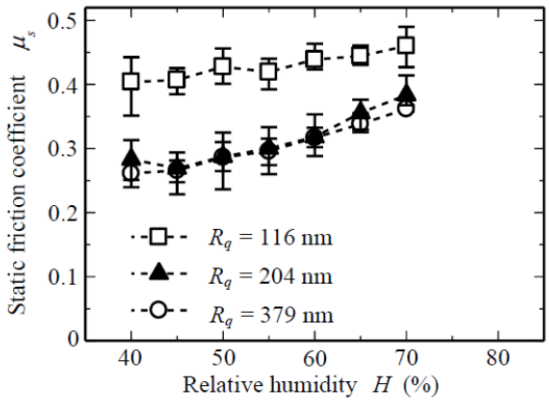

(a) T = 6 (N/m)

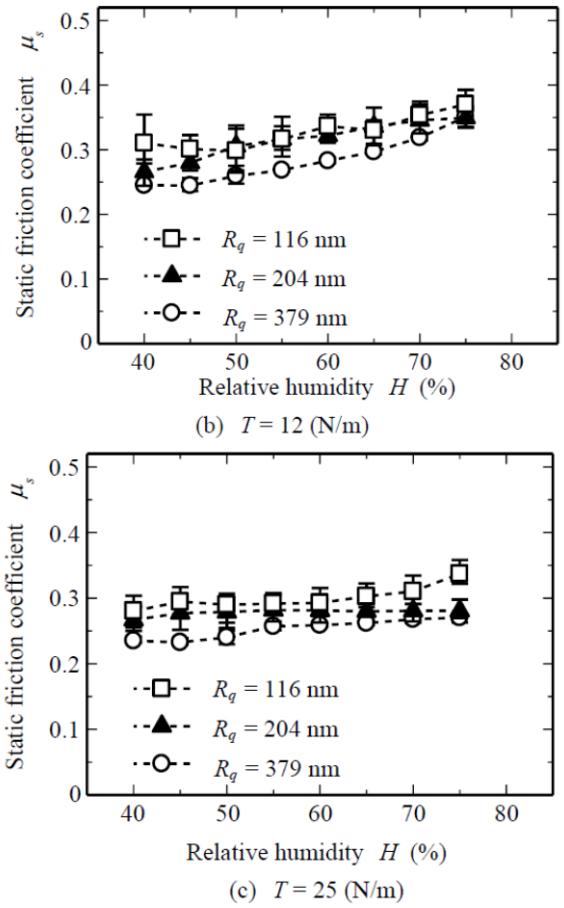

Figure 11 – Variation of static friction coefficient with relative humidity as a parameter of roller surface roughness

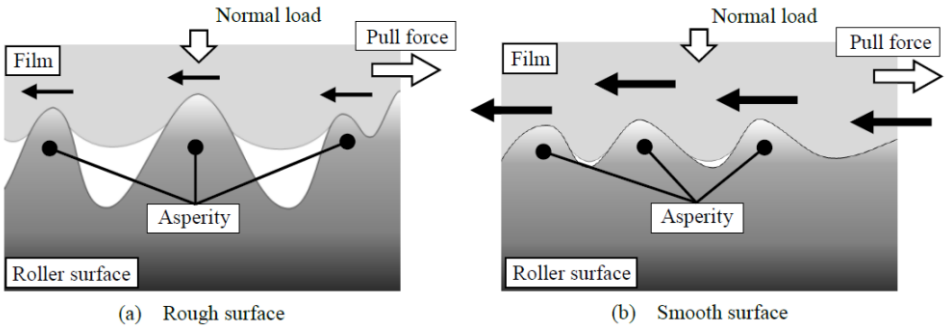

Figure 12 – Schematic diagram of interface between rough or smooth surface and film

Moreover, analysis of variance was conducted to determine the contribution ratio of each factor to static friction coefficient using these results. As a result, it was confirmed statistically that contribution ratio of three factors; relative humidity, web tension and

surface roughness are 23.8 %, 32.6 % and 36.1 %, were very high.

CONCLUSIONS

In this paper, the effect of each factors, film thickness, relative humidity, web tension and roller surface roughness, on static friction between the plastic film and steel roller was examined experimentally. The main conclusions are briefly summarized as follows:

(1) Film thickness has a significant effect on the static friction coefficient between plastic film and steel roller.
(2) The surface potential on the plastic film used for this experiment was generated within the range of -1.5 kV to 0 kV and there is no correlation between the static friction coefficient and static electricity.
(3) The static friction coefficient was increased with an increase in the relative humidity, and the tendency is similar to the results of meniscus force with relative humidity.
(4) The static friction coefficient in the case of thin film under low web tension using the roller with smooth surface roughness was significantly increased due to anchor effect and sagging effect between the deformed film and roller surface asperities.

As mentioned above, the static friction coefficient between the film and roller surface was significantly influenced by surrounding environment. Therefore, it is also highly possible that temperature affects the static friction coefficient because relative humidity correlates with temperature. The experiments on the effect of temperature on the static friction coefficient have been carried out with simultaneous control over temperature and relative humidity. Furthermore, it is important to investigate not only static friction coefficient but also kinetic friction coefficient when the environmental conditions were changed. It is planned to continue the task in order to also consider the kinetic friction experimentally.

REFERENCES

1. Hashimoto, H., "Theoretical and Experimental Investigation into Generation of Wrinkling and Slip in Plastic-Films under Transportation," JSME Journal of Advanced Mechanical Design, Systems, and Manufacturing, Vol. 4, No. 1, 2010, pp.238-248.
2. Hikita, S., and Hashimoto, H., "Improvement of Slippage and Wrinkling of Transporting Webs Using Micro-Grooved Rollers," JSME Journal of Advanced Mechanical Design, Systems, and Manufacturing, Vol. 4, No. 1, 2010, pp. 226-237.
3. Knox, K. L., and Sweency, T. L., "Fluid Effects Associated with Web Handling," Ind. Eng. Chem. Process Des. Develop., Vol. 10, No. 2, 1971, pp. 201-205.
4. Eshel, A., and Elrod, H. G., "The Theory of the Infinitely Wide, Perfectly Flexible, Self-Acting Foil Bearing," Trans. ASME, Journal of Lubr. Technol., 1965, pp. 92-97.
5. Ducotey, K.S., and Good, J.K., "The Importance of Traction in Web Handling," Trans. ASME, Journal of Tribology, Vol. 117, No. 4, 1995, pp. 679-684.
6. Ducotey, K. S., and Good, J. K., "The Effect of Web Permeability and Side Leakage on the Air Film Height between a Roller and Web," Trans. ASME, Journal of Tribology, Vol. 120, 1998, pp. 559-565.
7. Rice, B. S., Muftu, S., and Cole, K. A., "A Model for Determining the Asperity Engagement Height in Relation to Web Traction over Non-Vented Rollers," Trans. ASME, Journal of Tribology, Vol. 124, 2002, pp. 584-564.

8. Hashimoto, H., “Air Film Thickness Estimation in Web Handling Process,” Trans. ASME, Journal of Tribology, Vol. 121, 1999, pp. 50-55.
9. Hashimoto, H., and Nakagawa, H., “Improvement of Web Spacing and Friction Characteristics by Two Types of Stationary Guides,” Trans. ASME, Journal of Tribology, Vol. 123, 2001, pp. 509-516.
10. Patir, N., and Cheng, H. S., “An Average Flow model for Determining Effects of Three-Dimensional Roughness on Partial Hydrodynamic Lubrication,” Trans. ASME, Journal of Tribology, Vol. 100, 1978, pp. 12-17.
11. Hashimoto, H., and Okajima, M., “Theoretical and Experimental Investigations into Spacing Characteristics between Roller and Three Types of Webs with Different Permeabilities,” Trans. ASME, Journal of Tribology, Vol. 128, 2006, pp. 267-274.